Xi and Gao *Chin. J. Mech. Eng.* (2018) 31:15
https://doi.org/10.1186/s10033-018-0216-7

Chinese Journal of Mechanical Engineering

ORIGINAL ARTICLE

Open Access

Type Synthesis of Walking Robot Legs

Da Xi and Feng Gao*

Abstract

Walking robots use leg structures to overcome obstacles or move on complicated terrains. Most robots of current researches are equipped with legs of simple structure. The specific design method of walking robot legs is seldom studied. Based on the generalized-function (GF) set theory, a systematic type synthesis process of designing robot legs is introduced. The specific mobility of robot legs is analyzed to obtain two main leg types as the goal of design. Number synthesis problem is decomposed into two stages, actuation and constraint synthesis by name, corresponding to the combinatorics results of linear Diophantine equations. Additional restrictions are discussed to narrow the search range to propose practical limb expressions and kinematic-pair designs. Finally, all the fifty-one leg structures of four subtypes are carried out, some of which are chosen to make up robot prototypes, demonstrating the validity of the method. This paper proposed a novel type synthesis methodology, which could be used to systematically design various practical robot legs and the derived robots.

Keywords: Type synthesis, Robot leg, GF set, Number synthesis, Linear Diophantine equation

1 Introduction

Walking robots with multiple legs have been wildly applied to tough missions associated with uneven terrains. It is the leg structure that separates the body locomotion from the feet motion while overcoming obstacles. As a result, the body could maintain balance, leading to a good adaption of most common terrains. Walking robots become the hot spots recently at the leading edge of robot research. Various robot prototypes were tested with specific tasks, including BigDog [1, 2], FROG-I [3, 4], B-elepht [5, 6], Hector [7], Crabster [8–11], PPHex [12–14] and many other biomechanics [15, 16]. Legs are the key parts of the walking robot structure. On the one hand, exquisitely-designed legs make it possible to match the corresponding control algorithm to achieve high operating efficiency [17]. On the other hand, most of the leg designs in up-to-date researches are simply of serial structure or of pantograph mechanism [18]. The oversimplified type of legs, to a certain extent, increases difficulty in gait controlling or mechanism protecting. A specific type synthesis method of designing walking robot legs is a powerful tool for improving the operating performance.

Type synthesis is fundamental to mechanism design. The types of the mechanisms primarily determine several basic characters, such as the degree of freedom (DoF), coupling relation between input and output, singularity, workspace. A large number of researchers have done tremendous work on type synthesis, especially the relative difficult topics on parallel mechanisms. Many theoretical synthesis methods have been proposed and applied on numerous mechanisms basic on various mathematical concepts, such as differential manifolds [19], translational topology [20], screw theory [21], set theory [22]. But in previous literatures, few of them has been involved in systematic design of walking robot legs.

The theory of generalized-function sets (GF set theory) was proposed by Gao et al. [23], to mathematically express the topological-performance property of the end-effectors of robotic mechanisms. The sequence and interaction effects between rotational and translational DoF of the end-effector were analyzed to describe the exact kinematic mobility. GF set theory was applied in type synthesis by Yang et al. [24], and Meng et al. [25, 26], where number synthesis formula and rules of operation were integrated. The systematic number synthesis solution, which led to the equation of structure parameters and end-effector characteristics, was creatively proposed

*Correspondence: gaofengsjtu@gmail.com
State Key Laboratory of Mechanical System and Vibration, Shanghai Jiao Tong University, Shanghai 200240, China

in GF set theory to open up new possibilities for mechanism design.

Most of the robot legs in recent researches have no less than three DoF. Theoretically, the leg's end-effector (i.e., the foot) is capable of moving arbitrarily in 3-D environment only if it has, at least, three active DoF to locate itself. While other DoF (active or passive) could be used to adapt to changing terrains or handle jobs like a manipulator. For this reason, this paper uses a systematic type synthesis method for 3-DoF walking robot legs based on GF set theory. The typical results of the design process are classified into two main types and four subtypes by motion characteristics and connection types. The listed results in this paper could be further studied to be combined into whole walking robots. With matched control algorithm, these robots could achieve high operating performance. The main contributions of the paper are as follows.

(1) Two main types of robot legs are analyzed and proposed.
(2) The equivalent number-synthesis equations of actuations and constraints are analyzed and solved by corresponding solutions in combinatorial mathematics.
(3) Various restrictions are set in every stage of design process to realize a systematic type-synthesis method based on GF set theory, which has never been referred to in previous literatures.
(4) Deign results are listed by four subtypes, several examples of which are compared with available prototypes to demonstrate the validity of the method.

This paper is organized as follows. Section 2 sets the goals of synthesis, based on the analyses of the two main robot leg types. Section 3 provides the solutions of the number-synthesis equations of actuations and constraints, which determine the GF expressions of limbs in Section 4. Section 5 raises some recommended limb designs of kinematic pairs. Typical design results of different limbs are illustrated in Section 6. Section 7 gives the conclusions.

2 Analyses of the Leg Mobility

Walking robots realize space locomotion via discontinuous contact with ground. This specific motion requires at least three DoF which could be either translational or rotational despite the conditions as follows.

Translational condition: At least one translational DoF is required to adapt to the terrains (i.e., RRR excluded).

Spatial condition: 3-D mobility of the end-effector is required (i.e., planar 3-DoF mechanism excluded).

Based on above application requests as well as the relevant studies around the world, the DoF of legs could be divided into two main types.

Type R: The end-effector has RRT DoF, as shown in Figure 1(a). Two rotational DoF about the hip and one translational DoF along the leg appear to be low level of anisotropy in horizontal directions. This type of leg fits omnidirectional experimental platforms or highly stable manipulator robots, e.g., RAIBERT Hopper [17, 27] and PPHex [14].

Type T: The end-effector has RTT DoF, as shown in Figure 1(b). Foot moves in the sagittal plane which is located by an R DoF about the hip. The relatively high performance in the sagittal plane makes it a splendid biomimetic mechanism, e.g., BigDog [2] and HyQ [28].

Table 1 gives the 6-D GF expressions of the two main types. GF expression, such as $G^{\mathrm{II}}_{\mathrm{F14}}(\mathrm{R}_\alpha, \mathrm{R}_\beta, \mathrm{T}_\mathrm{a}, 0, 0, 0)$, means it is the fourteenth GF set of class II, with two rotational and one translational DoF. All the GF sets used in this paper are listed in Ref. [25].

3 Number Synthesis

In GF set theory, mechanism parameters should satisfy the following integrated number-synthesis equation [29], see Eq. (1):

$$\begin{cases} 2F_\mathrm{D} + Q_\mathrm{r} - C_\mathrm{o} - \sum_{i=1}^{N}(q_i - 1) + \sum_{i=1}^{N}(c_i - 1) = 6, \\ c_i \le 6 - F_\mathrm{D}, \quad q_i \le F_\mathrm{D} + Q_\mathrm{r}, \end{cases} \tag{1}$$

where F_D is the dimension of the end-effector's characteristics, i.e., the quantity of nonzero elements in the GF

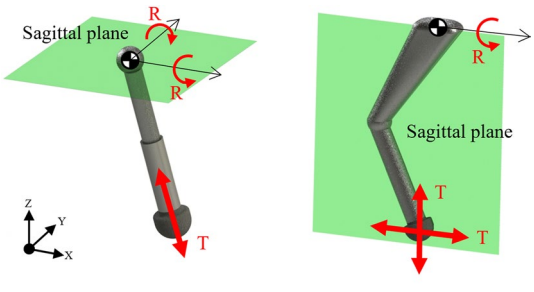

a Type R **b** Type T

Figure 1 Moving ability of the two main types of legs

Table 1 GF expressions of type R & type T

Type	End-effector's DoF	Condition
R	$G^{\mathrm{II}}_{\mathrm{F14}}(\mathrm{R}_\alpha, \mathrm{R}_\beta, \mathrm{T}_\mathrm{a}, 0, 0, 0)$	$\mathrm{R}_\alpha \nparallel \mathrm{R}_\beta$
T	$G^{\mathrm{II}}_{\mathrm{F16}}(\mathrm{R}_\alpha, \mathrm{T}_\mathrm{a}, \mathrm{T}_\mathrm{b}, 0, 0, 0)$	$\mathrm{R}_\alpha \perp \square \mathrm{T}_\mathrm{a}\mathrm{T}_\mathrm{b}$

set expression (F_D and DoF are equal in this paper); Q_r is the number of redundant actuations; C_o is the number of over-constraints; N is the total number of limbs; c_i is the number of constraints within the ith limb; q_i is the number of actuations within the ith limb.

Here we decompose Eq. (1) into two sub-equations for practical convenience. The end-effector's DoF, numbers of limbs and actuations should obey the actuation equation:

$$\begin{cases} N = F_D + Q_r - \sum_{i=1}^{N} (q_i - 1), \\ q_i \le F_D + Q_r. \end{cases} \tag{2}$$

The end-effector's DoF, numbers of limbs and constraints should obey the constrain equation:

$$\begin{cases} N = C_D + C_o - \sum_{i=1}^{N} (c_i - 1), \\ c_i \le C_D = 6 - F_D. \end{cases} \tag{3}$$

Limbs with total number N connect with each other in series, parallel or hybrid connection. It is worth mentioning that limbs connect in series or in parallel (actually series is a special case of parallel when $N = 1$) should obey Eqs. (2), (3) as a whole. While limbs in hybrid connection should obey the equations as local serial part or parallel part.

3.1 Number Synthesis of Actuations

Eq. (2) is the number-synthesis equation of actuations, where $q_i = 0$ indicates the limb is passive (i.e., without actuators). Passive limbs have two main specific impacts.

Constraining: Passive limbs provide constraints and rigidity to the end-effector if $c_i > 0$. The number of passive limb constraints is maximized in practice:

$$c_i = 6 - F_D,\ i \in \{i | q_i = 0\}. \tag{4}$$

Output: Passive limbs need not make room for actuator installation. Moreover, it has the same mobility as the end-effector if Eq. (4) is obeyed. As a result, it could be further designed to operate as the output of the leg (see more in Section 6).

In normal conditions, there is no more than one passive limb within the leg structure. Without loss of generality, set zero redundant actuation and Eq. (2) has the following equivalent form:

$$\begin{cases} \sum_{j=1}^{6} j \cdot n_{qj} = n_{q1} + 2n_{q2} + \ldots + 6n_{q6} = F_D, \\ \sum_{j=0}^{6} n_{qj} = n_{q0} + n_{q1} + n_{q2} + \ldots + n_{q6} = N, \end{cases} \tag{5}$$

where n_{qj} is the number of limbs with j actuations, $n_{q0} = 0, 1$.

Then we have:

$$N \le n_{q0} + F_D. \tag{6}$$

F_D is known as the goal of design. So far the solution of Eq. (5) could be expressed as an eight-dimension vector:

$$(N, n_{q0}, n_{q1}, n_{q2}, n_{q3}, n_{q4}, n_{q5}, n_{q6}). \tag{7}$$

Eq. (5) is called an constrained linear Diophantine Equation in combinatorics, solvability of which is included in Hilbert's tenth problem [30]. There have been numerous studies on this topic [31, 32]. In this paper, the solution Eq. (7) could be listed in sequence because of the specific parameters in the equation, and the analytical solving process is omitted.

Solutions of most common cases have been given in several articles of type synthesis [29, 33]. For parallel/serial legs, $\sum q_i = F_D = 3$, solutions are listed in Table 2, Q1–Q6. Similarly, for multi-DoF part in hybrid legs, the local parameters satisfy $\sum q_i = F_D = 2$. The local solutions are listed in Table 2, Q7–Q10.

3.2 Number Synthesis of Constraints

Similar to number synthesis of actuations, constraint Eq. (3) has the following equivalent form:

$$\begin{cases} \sum_{j=1}^{6} j \cdot n_{cj} = n_{c1} + 2n_{c2} + \ldots + 6n_{c6} = 6 - F_D + C_o, \\ \sum_{j=0}^{6} n_{cj} = n_{c0} + n_{c1} + n_{c2} + \ldots + n_{c6} = N, \end{cases} \tag{8}$$

where n_{cj} is the number of limbs with j constraints.

F_D and N are given as the design goal (Table 1) and the actuation number synthesis (Table 2), respectively. The solution of Eq. (8) could be expressed as an eight dimension vector:

$$(C_o, n_{c0}, n_{c1}, n_{c2}, n_{c3}, n_{c4}, n_{c5}, n_{c6}). \tag{9}$$

Table 2 Solutions of actuation number synthesis for parallel/serial legs

Index	[N, n_{qj}], j=0–6
Q1	[1,0,0,0,1,0,0,0]
Q2	[2,0,1,1,0,0,0,0]
Q3	[3,0,3,0,0,0,0,0]
Q4	[2,1,0,0,1,0,0,0]
Q5	[3,1,1,1,0,0,0,0]
Q6	[4,1,3,0,0,0,0,0]
Q7	[1,0,0,1,0,0,0,0]
Q8	[2,0,2,0,0,0,0,0]
Q9	[2,1,0,1,0,0,0,0]
Q10	[3,1,2,0,0,0,0,0]

The equations are analyzed for different types (see Table 1) and connections (parallel/serial, hybrid) in the rest of the section.

3.2.1 Type R in Parallel/Series (Type R-P)

According to the analysis at the beginning of Section 3, in the process of synthesis, connection in series is a special case of that in parallel when $N = 1$. So here **type R-P** represents legs of type R in both parallel and serial connections.

The end-effector's DoF is expressed in GF sets as $G^{II}_{F14}(R_\alpha, R_\beta, T_a, 0, 0, 0)$ in Table 1. The corresponding constraint condition is as follows.

Condition R0: The total constraints—two translational and one rotational constraints—are given in GF expression as $\overline{G_F}(\overline{T_b}, \overline{T_c}, \overline{R_\gamma}, 0, 0, 0)$.

The expression $G^{II}_{F14}(R_\alpha, R_\beta, T_a, 0, 0, 0)$, denotes **GF14**, belongs to the second class of GF sets [34]. Since GF14 has two incomplete rotations, leading to the analyses below.

Analysis 1: According to intersection rules, all the intersecting limbs should contain the end-effector's DoF. Table 3 gives the possible limb expressions.

Analysis 2: All the incomplete rotations should be coaxis if the limbs intersect. But this could easily raise interference problem during assembly as well as decrease the stiffness of the whole structure, which is to be avoided.

The above analyses give the following conditions.

Condition R1: GF expression of the end-effector is the intersection set of all the limbs' expressions.

Condition R2: Only one limb has two incomplete rotations as GF14.

Condition R3: Despite those referred to in Condition R2, rotations of limbs (if exist) must be complete.

All limb expressions meet Condition R3 have three translations, i.e., no translational constraints exist (see first two cases in Table 3). Therefore the only solution is that the two translational constraints in Condition R0 exist in the limbs of Condition R2, which comes to the condition below:

Condition R4: Only one translation is permitted in the limbs of Condition R2 (GF10, GF23 and GF 25 are all excluded).

All the candidate limbs are marked in Table 3.

Candidates in Table 3 give the restrictions of Eq. (8).

Firstly, either GF8 or GF14 must be chosen to be the most constrained limb, i.e., $n_{c2} + n_{c3} = 1$. In addition, passive limb (if exists) is the most constrained as Eq. (4) indicates, i.e.,

$$c_i = \max\{c\}, i \in \{i | q_i = 0\}. \tag{10}$$

Secondly, the only possible over-constraint is $\overline{R_\gamma}$, which comes to $C_o \le N - 1$.

The solutions are listed in Table 4.

Every group of limbs in Table 4 matches a proper actuation solution in Table 2.

Table 4 Solutions of constrain number synthesis for type R-P

Index	*N*	$[C_o, n_{cj}]$, $j = 0$–6
C-RP-1 (series)	1	[0,0,0,0,1,0,0,0]
C-RP-2	2	[0,1,0,0,1,0,0,0]
C-RP-3	2	[0,0,1,1,0,0,0,0]
C-RP-4	2	[1,0,1,0,1,0,0,0]
C-RP-5	3	[0,2,0,0,1,0,0,0]
C-RP-6	3	[0,1,1,1,0,0,0,0]
C-RP-7	3	[1,1,1,0,1,0,0,0]
C-RP-8	3	[1,0,2,1,0,0,0,0]
C-RP-9	3	[2,0,2,0,1,0,0,0]
C-RP-10	4	[0,3,0,0,1,0,0,0]
C-RP-11	4	[0,2,1,1,0,0,0,0]
C-RP-12	4	[1,2,1,0,1,0,0,0]
C-RP-13	4	[1,1,2,1,0,0,0,0]
C-RP-14	4	[2,1,2,0,1,0,0,0]
C-RP-15	4	[2,0,3,1,0,0,0,0]
C-RP-16	4	[3,0,3,0,1,0,0,0]

Table 3 Intersection limb expressions of GF14

Limb expression	Rotation	Constraint	Candidate	Number limitation
$G^{I}_{F1}(T_a, T_b, T_c, R_\alpha, R_\beta, R_\gamma)$	Complete	$\overline{G_F}(0, 0, 0, 0, 0, 0)$	Y	/
$G^{I}_{F2}(T_a, T_b, T_c, R_\alpha, R_\beta, 0)$	Complete	$\overline{G_F}(\overline{R_\gamma}, 0, 0, 0, 0, 0)$	Y	/
$G^{I}_{F3}(T_a, T_b, T_c, R_\alpha, 0, 0)$	Incomplete	$\overline{G_F}(\overline{T_b}, \overline{T_c}, 0, 0, 0, 0)$	Y	< 2
$G^{II}_{F10}(R_\alpha, R_\beta, T_a, T_b, 0, 0)$	Incomplete	$\overline{G_F}(\overline{T_c}, \overline{R_\gamma}, 0, 0, 0, 0)$	N	/
$G^{II}_{F14}(R_\alpha, R_\beta, T_a, 0, 0, 0)$	Incomplete	$\overline{G_F}(\overline{T_b}, \overline{T_c}, \overline{R_\gamma}, 0, 0, 0)$	Y	< 2
$G^{III}_{F23}(R_\alpha, R_\beta, T_a, T_b, R_\gamma, 0)$	Partially complete	$\overline{G_F}(\overline{T_c}, 0, 0, 0, 0, 0)$	N	/
$G^{III}_{F25}(R_\alpha, T_a, T_b, R_\beta, 0, 0)$	Partially complete	$\overline{G_F}(\overline{T_c}, \overline{R_\gamma}, 0, 0, 0, 0)$	N	/

3.2.2 Type R in Hybrid Connection (Type R-H)

For every set of solution in Table 4, if one limb of which is decomposed into serial part and parallel part, a hybrid leg is synthesized, as shown in Figure 2. In particular, if one limb is multi-actuated, decomposition to hybrid connection would rearrange its actuators. The location of the actuators is optimized to get a lower inertia and higher stiffness. For this reason, transformation into hybrid form changes the actuations and limb structures, which takes advantage of both series and parallel connections.

For type R-P, the total number of actuations is $\sum q_i = F_D = 3$, which indicates the existence of multi-actuation limb in Table 4 if $N < 3$. Here this multi-actuation limb is chosen to take a DoF rearrangement to transform into hybrid form.

If $N = 1$, it is exactly serially connected. The high isotropy in horizontal directions requires the equally good performance of the two rotational pairs. Hence the rotations are transformed to parallel here:

$$\begin{aligned} &G^{II}_{F14}(R_\alpha, R_\beta, T_a, 0, 0, 0) \\ &\quad = \text{parallel } G^{II}_{F18}(R_\alpha, R_\beta, 0, 0, 0, 0) \\ &\qquad \cup \text{series } G^{I}_{F7}(T_a, 0, 0, 0, 0, 0). \end{aligned} \tag{11}$$

Similar to type R-P, the parallel part of hybrid limb, GF18, has two incomplete rotational DoF. Considering analyses R1–R4 for type R-P, candidate limbs are derived from a similar process, see Table 5.

Here the local DoF $F_D = 2$. In addition, the spatial rotational ability of GF18 requires 3-D stability, suggesting at least 3 limbs. Then local passive limb is included that $n_{q0} = 1$. Take the equal sign in Eq. (6) so that $N = 3$.

The solutions are listed in Table 6.

Every group of limbs in Table 6 matches a two-actuation solution, Q10 in Table 2. Another actuation is left for the serial part GF7 in Eq. (11).

If $N = 2$, the more constrained limb restricts the end-effector's mobility. Consequently, it sustains larger constraining force. Here this limb is chosen to be the passive one according to Eq. (10). Thus the other actuating limb with less constraints is to be decomposed into hybrid form.

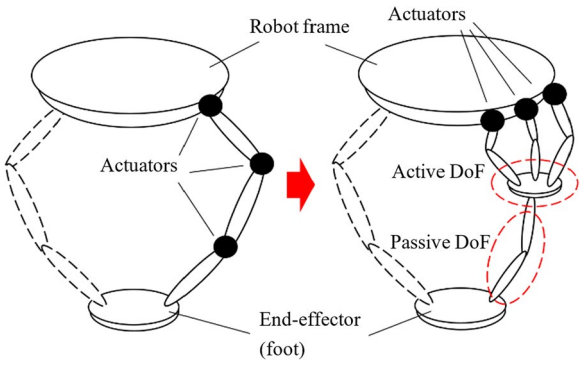

Figure 2 Decomposition of a leg into hybrid connection

Table 5 Candidate limbs of GF18

Limb expression	No. of cons.	Cons.	Lim.
$G^{II}_{F12}(R_\alpha, R_\beta, R_\lambda, 0, 0, 0)$	3	$\overline{G_F}(\overline{T_a}, \overline{T_b}, \overline{T_c}, 0, 0, 0)$	< 2
$G^{II}_{F18}(R_\alpha, R_\beta, 0, 0, 0, 0)$	4	$\overline{G_F}(\overline{T_a}, \overline{T_b}, \overline{T_c}, \overline{R_\gamma}, 0, 0)$	< 2
$G^{I}_{F1}(T_a, T_b, T_c, R_\alpha, R_\beta, R_\gamma)$	0	$\overline{G_F}(0, 0, 0, 0, 0, 0)$	/
$G^{I}_{F2}(T_a, T_b, T_c, R_\alpha, R_\beta, 0)$	1	$\overline{G_F}(\overline{R_\gamma}, 0, 0, 0, 0, 0)$	/

Table 6 Solutions of constrain number synthesis for GF18

Index	*N*	$[C_o, n_{cj}], j$=0–6
C-RH-1	3	[0,2,0,0,0,1,0,0]
C-RH-2	3	[0,1,1,0,1,0,0,0]
C-RH-3	3	[1,1,1,0,0,1,0,0]
C-RH-4	3	[1,0,2,0,1,0,0,0]
C-RH-5	3	[2,0,2,0,0,1,0,0]

Referring to Table 3, the actuating limb for $N = 2$ in Table 4 is expressed as GF1 (6-DoF) or GF2 (5-DoF), indicates that the total DoF of the single limb (local F_D) is more than the number of actuations. The difference of local F_D and actuation quantity is called passive DoF, which must be constrained by the passive limb. Generally, the passive DoF locates at the end of the limb. The passive DoF could be easily integrated into one kinematic pair, as the serial part of the hybrid limb. In the case here, rotations of GF1 or GF2 (see Table 3) are selected to be the passive DoF, operating as a universal joint or a spherical joint (see Section 5).

If the passive 2-rotational DoF (GF18 as a universal joint, see C-RP-3/4 in Table 4) is implemented, a 3-translational DoF (GF4) is required to get the specific characteristic of the end-effector:

$$\begin{aligned} &G^{I}_{F2}(T_a, T_b, T_c, R_\alpha, R_\beta, 0) \\ &\quad = \text{parallel } G^{I}_{F4}(T_a, T_b, T_c, 0, 0, 0) \\ &\qquad \cup \text{series } G^{II}_{F18}(R_\alpha, R_\beta, 0, 0, 0, 0). \end{aligned} \tag{12}$$

Pure multi-translational limb as GF4 is relatively complex in structure, and easily to import assembly error or interference problem. The design process here applies only one pure 3-translational limb. All the candidate limbs are listed in Table 7, using similar GF-set-theory analyses in Section 3.2.1.

Here the local DoF F_D=3 and the local passive limb is not included that $n_{q0} = 0$. Take the equal sign in Eq. (6)

Table 7 Candidate limbs of GF4

Limb expression	No. of cons.	Cons.	Lim.
$G^{I}_{F4}(T_a, T_b, T_c, 0, 0, 0)$	3	$\overline{G_F}(\overline{R_\alpha}, \overline{R_\beta}, \overline{R_\gamma}, 0, 0, 0)$	1
$G^{I}_{F1}(T_a, T_b, T_c, R_\alpha, R_\beta, R_\gamma)$	0	$\overline{G_F}(0, 0, 0, 0, 0, 0)$	/
$G^{I}_{F2}(T_a, T_b, T_c, R_\alpha, R_\beta, 0)$	1	$\overline{G_F}(\overline{R_\gamma}, 0, 0, 0, 0, 0)$	/
$G^{I}_{F3}(T_a, T_b, T_c, R_\alpha, 0, 0)$	2	$\overline{G_F}(\overline{R_\beta}, \overline{R_\gamma}, 0, 0, 0, 0)$	/

so that N=3. The solutions are listed in Table 8. Every group of limbs in Table 8 matches a three-actuation solution, Q3 in Table 2.

If the passive 3-rotational DoF (GF12 as a spherical joint, see GF1 in Table 3 and C-RP-2 in Table 4) is implemented, all GF sets with spatial mobility are equivalent to the 3-translational limb GF4, see the decomposition expressions below:

$$G^{I}_{F1}(T_a, T_b, T_c, R_\alpha, R_\beta, R_\gamma) =$$

$$G^{I}_{F4}(T_a, T_b, T_c, 0, 0, 0) \cup G^{II}_{F12}(R_\alpha, R_\beta, R_\lambda, 0, 0, 0) = \quad (13)$$

$$G^{II}_{F14}(R_\alpha, R_\beta, T_a, 0, 0, 0) \cup G^{II}_{F12}(R_\alpha, R_\beta, R_\lambda, 0, 0, 0) = \quad (14)$$

$$G^{II}_{F16}(R_\alpha, T_a, T_b, 0, 0, 0) \cup G^{II}_{F12}(R_\alpha, R_\beta, R_\lambda, 0, 0, 0). \quad (15)$$

Take the isotropy of type R into consideration, Eq. (14) is implemented as the same form as the passive limb (GF14 of case C-RP-2 in Table 4). The results have been listed already, see $N = 3$ cases in Table 4. Every group of which matches a three-actuation solution, Q3 in Table 2.

Above all analyses in this subsection, it is easily concluded that synthesis of hybrid structure could be transformed to those of parallel/series connections.

3.2.3 Type T in Parallel/Series Connections (Type T-P)

The end-effector's DoF is expressed in GF sets as GF16 (Table 1). The corresponding constraint condition is as follows.

Condition T0: The total constraints of the end-effector is given in GF expression as $\overline{G_F}(\overline{T_c}, \overline{R_\beta}, \overline{R_\gamma}, 0, 0, 0)$, which has one translational and two rotational constraints.

The expression GF16 belongs to the second class of GF sets like GF14 (Section 3.2.1). The incomplete rotation in GF16 imply the similar analyses of condition R1–R4 in Section 3.2.1. The counterpart candidate limbs are listed in Table 9.

Table 9 imposes restrictions on Eq. (8). Firstly, if GF16 is excluded in a synthesis, then both GF10 and GF3 should be implemented together to constrain $\overline{T_c}$ and $\overline{R_\beta}$, i.e., $n_{c2} \geq 2$, *if* $n_{c3} = 0$. Secondly, either $\overline{R_\beta}$or $\overline{R_\gamma}$ could be over-constrained that $C_o \leq 2(N-1)$.

The solutions are listed in Table 10, each group of which matches a proper actuation solution in Table 2.

Table 8 Solutions of constrain number synthesis for GF4

Index	*N*	$[C_o, n_{cj}]$, *j*=0–6
C-RH-6	3	[0,2,0,0,1,0,0,0]
C-RH-7	3	[1,1,1,0,1,0,0,0]
C-RH-8	3	[2,1,0,1,1,0,0,0]
C-RH-9	3	[2,0,2,0,1,0,0,0]
C-RH-10	3	[3,0,1,1,1,0,0,0]
C-RH-11	3	[4,0,0,2,1,0,0,0]

Table 9 Candidate limbs of type T-P

Limb expression	No. of cons.	Cons.	Lim.
$G^{II}_{F10}(R_\alpha, R_\beta, T_a, T_b, 0, 0)$	2	$\overline{G_F}(\overline{T_c}, \overline{R_\gamma}, 0, 0, 0, 0)$	< 2
$G^{II}_{F16}(R_\alpha, T_a, T_b, 0, 0, 0)$	3	$\overline{G_F}(\overline{T_c}, \overline{R_\beta}, \overline{R_\gamma}, 0, 0, 0)$	< 2
$G^{I}_{F1}(T_a, T_b, T_c, R_\alpha, R_\beta, R_\gamma)$	0	$\overline{G_F}(0, 0, 0, 0, 0, 0)$	/
$G^{I}_{F2}(T_a, T_b, T_c, R_\alpha, R_\beta, 0)$	1	$\overline{G_F}(\overline{R_\gamma}, 0, 0, 0, 0, 0)$	/
$G^{I}_{F3}(T_a, T_b, T_c, R_\alpha, 0, 0)$	2	$\overline{G_F}(\overline{R_\beta}, \overline{R_\gamma}, 0, 0, 0, 0)$	/

3.2.4 Type T in Hybrid Connection (Type T-H)

Similar to type R-H in Section 3.2.2, solutions of $N < 3$ in Table 10 show the feasibility of transformation into hybrid limbs. Choose the most-actuated limb to be decomposed into serial and parallel parts.

If N=1, it is exactly serially connected. Take into consideration the high performance in sagittal plane of type-T leg, the two translational DoF in the plane are transformed to be the parallel part:

$$\begin{aligned} &G^{II}_{F16}(R_\alpha, T_a, T_b, 0, 0, 0) \\ &\quad = \text{series } G^{II}_{F21}(R_\alpha, 0, 0, 0, 0, 0) \\ &\quad \cup \text{parallel } G^{I}_{F6}(T_a, T_b, 0, 0, 0, 0). \end{aligned} \quad (16)$$

For planer mechanism, to increase stiffness and to reduce the unnecessary kinematic pairs, only planer limbs are considered here without local passive ones [35, 36]. Here are two candidates listed in Table 11. The solutions are listed in Table 12. Every group of limbs matches a two-actuation solution, Q8 in Table 2. Another actuation is left for the series part GF21 in Eq. (16).

If $N = 2$, referring to the analyses of type R-H in Section 3.2.2, the more constrained limb is chosen to be passive. The other actuating limb is to be decomposed into hybrid form.

Referring to Table 9, the actuating limb for N=2 in Table 10 is expressed as GF1 (6-DoF), GF2 (5-DoF), or GF3 (4-DoF), indicates that the total DoF of the single limb (local F_D) is more than the number of actuations. Here we again combine the rotations of the limbs into

Table 10 Solutions of constrain number synthesis for type T-P

Index	*N*	$[C_o, n_{ci}]$, $j = 0$–6
C-TP-1 (series)	1	[0,0,0,0,1,0,0,0]
C-TP-2	2	[0,1,0,0,1,0,0,0]
C-TP-3	2	[1,0,1,0,1,0,0,0]
C-TP-4	2	[1,0,0,2,0,0,0,0]
C-TP-5	2	[2,0,0,1,1,0,0,0]
C-TP-6	3	[0,2,0,0,1,0,0,0]
C-TP-7	3	[1,1,1,0,1,0,0,0]
C-TP-8	3	[1,1,0,2,0,0,0,0]
C-TP-9	3	[2,1,0,1,1,0,0,0]
C-TP-10	3	[2,0,2,0,1,0,0,0]
C-TP-11	3	[2,0,1,2,0,0,0,0]
C-TP-12	3	[3,0,1,1,1,0,0,0]
C-TP-13	3	[3,0,0,3,0,0,0,0]
C-TP-14	3	[4,0,0,2,1,0,0,0]
C-TP-15	4	[0,3,0,0,1,0,0,0]
C-TP-16	4	[1,2,1,0,1,0,0,0]
C-TP-17	4	[1,2,0,2,0,0,0,0]
C-TP-18	4	[2,2,0,1,1,0,0,0]
C-TP-19	4	[2,1,2,0,1,0,0,0]
C-TP-20	4	[2,1,1,2,0,0,0,0]
C-TP-21	4	[3,1,1,1,1,0,0,0]
C-TP-22	4	[3,0,3,0,1,0,0,0]
C-TP-23	4	[3,1,0,3,0,0,0,0]
C-TP-24	4	[3,0,2,2,0,0,0,0]
C-TP-25	4	[4,1,0,2,1,0,0,0]
C-TP-26	4	[4,0,2,1,1,0,0,0]
C-TP-27	4	[4,0,1,3,0,0,0,0]
C-TP-28	4	[5,0,1,2,1,0,0,0]
C-TP-29	4	[5,0,0,4,0,0,0,0]
C-TP-30	4	[6,0,0,3,1,0,0,0]

Table 11 Candidate limbs of GF6

Limb expression	No. of cons.	Cons.	Lim.
$G^{I}_{F5}(T_a,T_b,R_\alpha,0,0,0)$ $(R_\alpha \perp \square T_a,T_b)$	3	$\overline{G_F}(\overline{R_\beta},\overline{R_\gamma},\overline{T_c},0,0,0)$	< 2
$G^{I}_{F6}(T_a,T_b,0,0,0,0)$	4	$\overline{G_F}(\overline{R_\alpha},\overline{R_\beta},\overline{R_\gamma},\overline{T_c},0,0,0)$	< 2

Table 12 Solutions of constrain number synthesis for GF6

Index	*N*	$[C_o, n_{ci}]$, $j = 0$–6
C-TH-1 (series)	2	[3,0,0,0,1,1,0,0]
C-TH-2	2	[4,0,0,0,0,2,0,0]

passive joints. The problem is transformed to 3-DoF mechanism synthesis. The union formula goes as below:

$$\begin{aligned} &G^{I}_{F1}(T_a,T_b,T_c,R_\alpha,R_\beta,R_\gamma) \\ &\quad = G^{II}_{F16}(R_\alpha,T_a,T_b,0,0,0) \\ &\qquad \cup G^{II}_{F12}(R_\alpha,R_\beta,R_\lambda,0,0,0), \end{aligned} \tag{17}$$

$$\begin{aligned} &G^{I}_{F2}(T_a,T_b,T_c,R_\alpha,R_\beta,0) \\ &\quad = G^{I}_{F4}(T_a,T_b,T_c,0,0,0) \\ &\qquad \cup G^{II}_{F18}(R_\alpha,R_\beta,0,0,0,0), \end{aligned} \tag{18}$$

$$\begin{aligned} &G^{I}_{F3}(T_a,T_b,T_c,R_\alpha,0,0) \\ &\quad = G^{I}_{F4}(T_a,T_b,T_c,0,0,0) \\ &\qquad \cup G^{II}_{F21}(R_\alpha,0,0,0,0,0). \end{aligned} \tag{19}$$

Decomposition Eq. (17) requires to synthesize GF16, which is already done in Table 10 ($N = 3$ cases). Decomposition Eqs. (18), (19) require to synthesize GF4, which is listed in Table 8.

4 Limb Decomposition and Expression

Results of number synthesis are listed in Tables 4, 6, 8, 10, 12, each of which corresponds to one or more GF expressions in Tables 3, 5, 7, 9 and 11. If a mapping like this satisfies the restricted conditions below, it would represent a valid limb decomposition.

Condition 4.1: Intersection rules of GF sets (as shown in the "Condition" column of Tables 13, 14, 15, 16) [33]. The rules are about axes' locations of associated DoF between limbs, which were ever discussed in conditions R1–R4 in Section 3.2.

Condition 4.2: Other considerations based on practical use, including assembly interference (condition R2 and R3 in Section 3.2), structure stability (discussions in Sections 3.2.2 and 3.2.4), spatial symmetry, etc.

It is worth mentioning that, theoretically, the first condition above is necessary while the second is not. The unnecessary condition should be practically analyzed to find the required synthesis solutions in a relatively small search range.

Generally, legged robots have symmetric mobility. Here we take the symmetric limb expressions as examples, and set $N \geq 3$ for spatial parallel mechanisms (or parallel part of hybrid legs). For the rest results, the expressing process is similar and omitted here.

For different leg mobility characteristics (Table 1), the qualified limb expressions are listed in Tables 13, 14, 15, 16. $\| R^j_\alpha$ or $\| T^j_a$ means all the specified rotational or translational DoF axes in limbs j are parallel to each

Table 13 Limb expression for type R-P (referring Table 4)

N	Limb 1	Limb 2	Limb 3	Limb 4	Condition	Index
1	GF14	/	/	/	/	C-RP-1
3	GF14	GF1	GF1	/	/	C-RP-5
3	GF8	GF2	GF2	/	$\parallel R_{\alpha}^{j}, \parallel R_{\beta}^{j}, j = 2,3$	C-RP-8
3	GF14	GF2	GF2	/	$\parallel R_{\alpha}^{j}, \parallel R_{\beta}^{j}, j = 1,2,3$	C-RP-9
4	GF14	GF1	GF1	GF1	/	C-RP-10
4	GF8	GF2	GF1	GF1	/	C-RP-11
4	GF14	GF2	GF1	GF1	$\parallel R_{\alpha}^{j}, \parallel R_{\beta}^{j}, j = 1,2$	C-RP-12
4	GF8	GF2	GF2	GF1	$\parallel R_{\alpha}^{j}, \parallel R_{\beta}^{j}, j = 2,3$	C-RP-13
4	GF14	GF2	GF2	GF1	$\parallel R_{\alpha}^{j}, \parallel R_{\beta}^{j}, j = 1,2,3$	C-RP-14
4	GF8	GF2	GF2	GF2	$\parallel R_{\alpha}^{j}, \parallel R_{\beta}^{j}, j = 2,3,4$	C-RP-15
4	GF14	GF2	GF2	GF2	$\parallel R_{\alpha}^{j}, \parallel R_{\beta}^{j}, j = 1,2,3,4$	C-RP-16

Table 14 Limb expression for type R-H (referring Tables 4, 6 and 8)

Parallel limb 1	Parallel limb 2	Parallel limb 3	Serial limb	Other limb	Condition	Index
GF18	GF1	GF1	GF7	/	/	C-RH-1, C-RP-1
GF12	GF2	GF2	GF7	/	$\parallel R_{\alpha}^{j}, \parallel R_{\beta}^{j}, j = 2,3$	C-RH-4, C-RP-1
GF18	GF2	GF2	GF7	/	$\parallel R_{\alpha}^{j}, \parallel R_{\beta}^{j}, j = 1,2,3$	C-RH-5, C-RP-1
GF4	GF1	GF1	GF18	GF8/GF14	$\parallel R_{\alpha}^{j}, \parallel R_{\beta}^{j}, j = 4,5$	C-RH-6, C-RP-3/ C-RP-4
GF4	GF2	GF2	GF18	GF8/GF14	$\parallel R_{\alpha}^{j}, \parallel R_{\beta}^{j}, j = 4,5$	C-RH-9, C-RP-3/ C-RP-4
GF4	GF3	GF3	GF18	GF8/GF14	$\parallel R_{\alpha}^{j}, \parallel R_{\beta}^{j}, j = 4,5$	C-RH-11, C-RP-3/ C-RP-4
GF14	GF1	GF1	GF12	GF14	/	C-RP-5, C-RP-2
GF8	GF2	GF2	GF12	GF14	$\parallel R_{\alpha}^{j}, \parallel R_{\beta}^{j}, j = 2,3$	C-RP-8, C-RP-2
GF14	GF2	GF2	GF12	GF14	$\parallel R_{\alpha}^{j}, \parallel R_{\beta}^{j}, j = 1,2,3$	C-RP-9, C-RP-2

other. The indexes in the last column indicate the number synthesis in referred tables (Section 3).

5 Limb Design

A specific kinematic limb is designed by deciding the type, quantity and consequence of various kinematic pairs, which is based on the relation between the end-effector's mobility and the kinematic-pair axes.

Kinematic pairs include simple pairs and composite ones [33], see Table 17. Composite pairs assemble linkages with simple pairs to get compact multi-DoF units.

Using composite pairs in Table 17 and intersection rules of GF sets (e.g., Eqs. (11)–(19)), it is convenient to simplify the limb design, as well as to improve the structure stiffness, stability, etc. Table 18 lists the GF expressions employed in this paper, and the suggested compact kinematic limb designs as well. The subscript "//" or "//" in Table 18 means the rotation axes are parallel or unparalleled.

Actuation matching is another topic in robot design. In type synthesis stage, we focus on the total numbers and assembly locations of the actuators in a limb. The actuation numbers are matched during the discussion about Tables 4, 6, 8, 10 and 12 in Section 3. The actuation locations are underlined in the last column of Table 18. Different actuation systems could convert to each other for practical use, e.g., translational actuators could output rotations via linkage-slider mechanisms, while rotors could output translations by means of screws, see prototypes in the next section.

Table 15 Limb expression for type T-P (referring Table 10)

N	Limb 1	Limb 2	Limb 3	Limb 4	Condition	Index
1	GF16	/	/	/	/	C-TP-1
3	GF16	GF1	GF1	/		C-TP-6
3	GF16	GF2	GF2	/	$\parallel R_{\alpha}^{j}, j=1,2,3$	C-TP-10
3	GF10	GF3	GF3	/	$\parallel R_{\alpha}^{j}, j=1,2,3$	C-TP-13
3	GF16	GF3	GF3	/	$\parallel R_{\alpha}^{j}, j=1,2,3$	C-TP-14
4	GF16	GF1	GF1	GF1	/	C-TP-15
4	GF16	GF2	GF1	GF1	$\parallel R_{\alpha}^{j}, j=1,2$	C-TP-16
4	GF10	GF3	GF1	GF1	$\parallel R_{\alpha}^{j}, j=1,2$	C-TP-17
4	GF16	GF3	GF1	GF1	$\parallel R_{\alpha}^{j}, j=1,2$	C-TP-18
4	GF16	GF2	GF2	GF1	$\parallel R_{\alpha}^{j}, j=1,2,3$	C-TP-19
4	GF16	GF2	GF2	GF2	$\parallel R_{\alpha}^{j}, j=1,2,3,4$	C-TP-22
4	GF10	GF3	GF3	GF1	$\parallel R_{\alpha}^{j}, j=1,2,3$	C-TP-23
4	GF10	GF3	GF2	GF2	$\parallel R_{\alpha}^{j}, j=1,2,3,4$	C-TP-24
4	GF16	GF3	GF3	GF1	$\parallel R_{\alpha}^{j}, j=1,2,3$	C-TP-25
4	GF16	GF3	GF2	GF2	$\parallel R_{\alpha}^{j}, j=1,2,3,4$	C-TP-26
4	GF10	GF3	GF3	GF2	$\parallel R_{\alpha}^{j}, j=1,2,3,4$	C-TP-27
4	GF16	GF3	GF3	GF2	$\parallel R_{\alpha}^{j}, j=1,2,3,4$	C-TP-28
4	GF10	GF3	GF3	GF3	$\parallel R_{\alpha}^{j}, j=1,2,3,4$	C-TP-29
4	GF16	GF3	GF3	GF3	$\parallel R_{\alpha}^{j}, j=1,2,3,4$	C-TP-30

Table 16 Limb expression for type T-H (referring Tables 8, 10 and 12)

Parallel limb 1	Parallel limb 2	Parallel limb 3	Serial limb	Other limb	Condition	Index
GF21	GF6	GF5	/	/	$\parallel \square T_a^j T_b^j, j=2,3$	C-TH-1, C-TP-1
GF21	GF6	GF6	/	/	$\parallel \square T_a^j T_b^j, j=2,3$	C-TH-2, C-TP-1
GF12	GF16	GF1	GF1	GF16	/	C-TP-6, C-TP-2
GF12	GF16	GF2	GF2	GF16	$\parallel R_{\alpha}^{j}, j=2,3,4$	C-TP-10, C-TP-2
GF12	GF10	GF3	GF3	GF16	$\parallel R_{\alpha}^{j}, j=2,3,4$	C-TP-13, C-TP-2
GF12	GF16	GF3	GF3	GF16	$\parallel R_{\alpha}^{j}, j=2,3,4$	C-TP-14, C-TP-2
GF18	GF4	GF1	GF1	GF16	$\parallel R_{\alpha}^{j}, j=1,5$	C-RH-6, C-TP-3
GF18	GF4	GF2	GF2	GF16	$\parallel R_{\alpha}^{j}, j=1,5$	C-RH-9, C-TP-3
GF18	GF4	GF3	GF3	GF16	$\parallel R_{\alpha}^{j}, j=1,5$	C-RH-11, C-TP-3
GF21	GF4	GF1	GF1	GF10/GF16	$\parallel R_{\alpha}^{j}, j=1,5$	C-RH-6, C-TP-4/ C-TP-5
GF21	GF4	GF2	GF2	GF10/GF16	$\parallel R_{\alpha}^{j}, j=1,5$	C-RH-9, C-TP-4/ C-TP-5
GF21	GF4	GF3	GF3	GF10/GF16	$\parallel R_{\alpha}^{j}, j=1,5$	C-RH-11, C-TP-4/ C-TP-5

6 Examples of Synthesis Results

For each limb expression in Section 4, take the corresponding kinematic form in Section 5 to get a final type of walking robot leg. Here several typical examples of the four subtypes (i.e., type R-P, R-H, T-P and T-H) are illustrated and compared with some real robots to show the validity of the synthesis methodology. Actuators, joints, robot frames and fixed adjacent linkages are distinguished by colors.

Table 17 GF expressions of kinematic pairs used in this paper

Kinematic pair	Symbol	DoF	GF expression
Prismatic pair	P	1	$G^{I}_{F7}(T_a,0,0,0,0,0)$
Revolute pair	R	1	$G^{II}_{F21}(R_\alpha,0,0,0,0,0)$
Cylinder pair	C	2	$G^{II}_{F20}(T_a,R_\alpha,0,0,0,0)$
Spherical pair	S	3	$G^{II}_{F12}(R_\alpha,R_\beta,R_\gamma,0,0,0)$
Universal pair	U	2	$G^{II}_{F18}(R_\alpha,R_\beta,0,0,0,0)$
T-R universal pair	U^	2	$G^{II}_{F20}(T_a,R_\alpha,0,0,0,0)$
R-T universal pair	^U	2	$G^{II}_{F19}(R_\alpha,T_a,0,0,0,0)$
Parallelogram pair	P^R	1	$G^{I}_{F7}(T_a,0,0,0,0,0)$

Table 18 Limb design of GF expressions

No.	Limb GF expression	DoF	Kinematic pair design
1	$G^{I}_{F1}(T_a,T_b,T_c,R_\alpha,R_\beta,R_\gamma)$	6	UPS, RUS
2	$G^{I}_{F2}(T_a,T_b,T_c,R_\alpha,R_\beta,0)$	5	RRU^R
3	$G^{I}_{F3}(T_a,T_b,T_c,R_\alpha,0,0)$	4	RRU^
4	$G^{I}_{F4}(T_a,T_b,T_c,0,0,0)$	3	P^U
5	$G^{I}_{F5}(T_a,T_b,R_\alpha,0,0,0)$	3	UR, $RRR_{//}$
6	$G^{I}_{F6}(T_a,T_b,0,0,0,0)$	2	PP
7	$G^{I}_{F7}(T_a,0,0,0,0,0)$	1	P
8	$G^{II}_{F8}(R_\alpha,R_\beta,R_\gamma,T_a,0,0)$	4	SP
9	$G^{II}_{F10}(R_\alpha,R_\beta,T_a,T_b,0,0)$	4	URR, URP, $RR_{//}$^U
10	$G^{II}_{F12}(R_\alpha,R_\beta,R_\lambda,0,0,0)$	3	S, $RRR_{//}$
11	$G^{II}_{F14}(R_\alpha,R_\beta,T_a,0,0,0)$	3	UP, $RR_{//}$P
12	$G^{II}_{F16}(R_\alpha,T_a,T_b,0,0,0)$	3	RPP, R^U, $RRR_{//}$
13	$G^{II}_{F18}(R_\alpha,R_\beta,0,0,0,0)$	2	U, $RR_{//}$
14	$G^{II}_{F21}(R_\alpha,0,0,0,0,0)$	1	R

6.1 Examples of Type R-P

Two examples of legs with RRT DoF in parallel/series are listed in Table 19.

Figure 3(a) illustrates the leg model in series, which is a simple and common case of type R-P. All kinematic pairs install actuators (present as brown discs or golden cylinders in Figure 3) to perform as a lightweight experimental platform. Passive DoF could be implemented between the foot and the ground to adapt to terrains. A famous typical robot using this kind of leg is the one-legged hopper by Raibert et al. [17].

Table 19 Example legs of type R-P

Connection	*N*	Limb 1	Limb 2	Limb 3	Index
Series	1	RRP	/	/	C-RP-1
Parallel	3	UP	UPS	UPS	C-RP-5

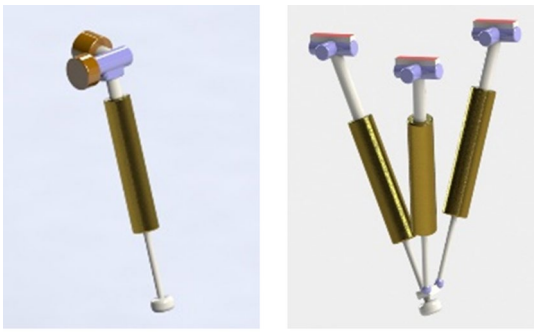

a serial limb **b** parallel limbs

Figure 3 Leg model of type R-P

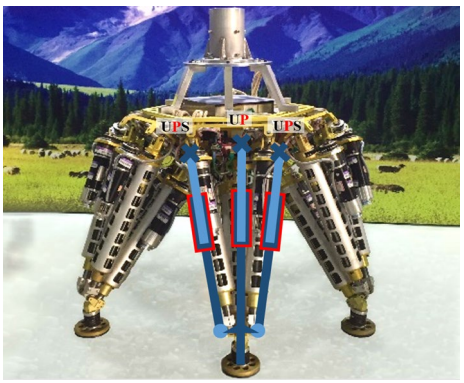

Figure 4 Six-legged robot of R-P legs

Figure 3(b) illustrates the second set in Table 19. Three actuators distributed on each parallel limb perform as muscles. Actuations are easily matched to get high load capacity. A six-legged robot prototype with isotropy in horizontal plane [13, 37] is shown in Figure 4, which was designed by the authors' research team.

6.2 Examples of Type R-H

Hybrid legs of type R-H take advantage of those in series and in parallel, which should be specifically designed in practice. Some examples are shown in Table 20.

Figure 5(a) illustrates the first example in Table 20, which is of 3-DoF hybrid limb. It is the basic hybrid form.

Table 20 Example legs for type R-H

Parallel limb 1	Parallel limb 2	Parallel limb 3	Serial limb	Other limb	Index
U	UPS	UPS	P	/	C-RH-1, C-RP-1
UP	UPS	UPS	RR(R)	UC	C-RP-5, C-RP-2

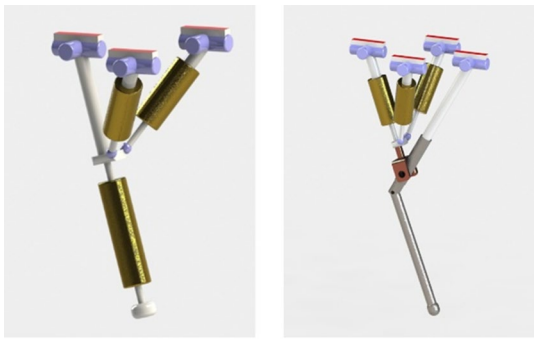

a 3-DoF **b** 6-DoF

Figure 5 Leg model of type R-H

Figure 5(b) illustrates the second set of leg in Table 20. It has a 6-DoF hybrid limb with a 3-DoF-active part and 3-DoF passive joints. The actuation part is isolated from the passive leg linkages to get better protection or insulation. In Figure 5(b), a revolute pair of the hybrid limb is integrated into the prismatic pair of the passive limb to combine a cylinder pair. A possible robot using this kind of leg is shown in Figure 6.

6.3 Examples of Type T-P

Examples of legs with RTT-DoF in parallel/series are listed in Table 21.

Figure 7(a) illustrates a simple serial model. The parallel revolute pairs perpendicular to the sagittal plane are used to substitute for the translational DoF.

Figure 7(b) introduces a type of one passive and three active limbs. Three active actuating "muscles" are centro-symmetric to improve the lateral performance. The actuators are installed separately from leg linkages to make it possible to work in extreme conditions (earthquake, fire, etc.). Passive prismatic pairs in the sagittal plane are replaced with a ^U pair. Corresponding walking robot model with this type of legs is shown in Figure 8.

Figure 6 Robot model of R-H legs

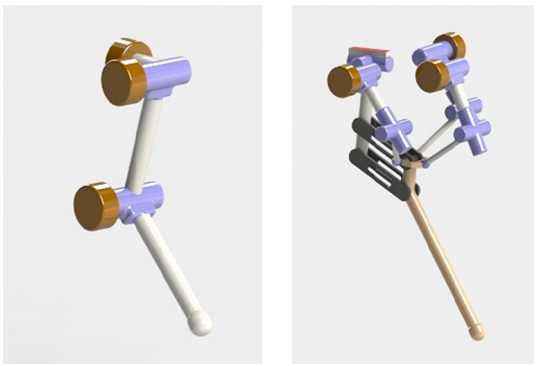

a Serial limb **b** Parallel limbs

Figure 7 Leg model of type T-P

6.4 Examples of Type T-H

Hybrid legs of type T derive from serial/parallel ones, see Table 22 for some examples.

Figure 9(a) shows the first model of 3-DoF hybrid limb in Table 22. The parallel revolute pairs are used to create the derivative translational characteristics in the sagittal plane. Figure 10 is a quadruped prototype using this kind of leg [6]. It was designed and tested by the authors'

Figure 8 Robot model of T-P legs

Table 21 Example legs for type T-P

Connection	*N*	Limb 1	Limb 2	Limb 3	Limb 4	Index
Series	1	RRR	/	/	/	C-TP-1
Parallel	4	R^U	RUS	RUS	RUS	C-TP-15

Table 22 Example legs for type T-H

Parallel limb 1	Parallel limb 2	Parallel limb 3	Serial limb	Other limb	Index
RR	RRR	/	R	/	C-TH-1, C-TP-1
RU	RUS	RUS	S	R^U	C-TP-6, C-TP-2

a 3-DoF **b** 6-DoF

Figure 9 Leg model of type T-H

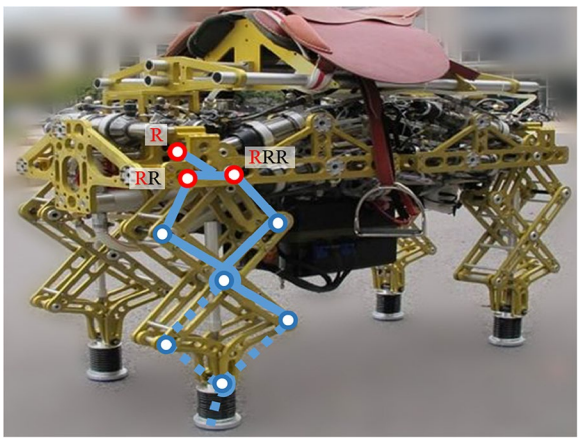

Figure 10 Quadruped BabyElephant of T-H legs

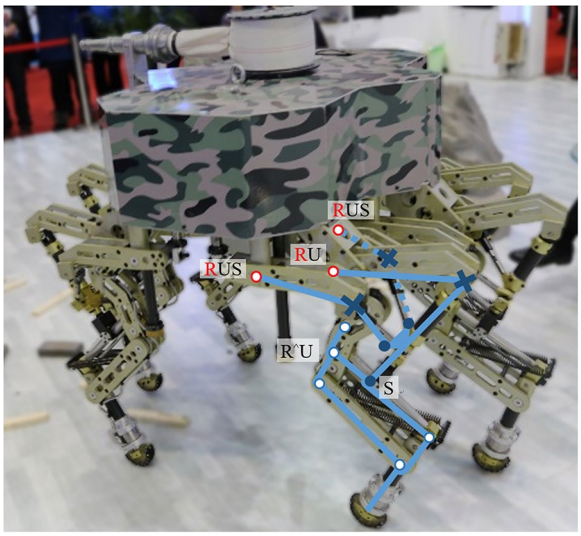

Figure 11 Hexapod robot of T-H legs

research group, leading by Prof. GAO. Additional parallel links are used to increase the planer rigidity.

Figure 9(b) shows the second model in Table 22 with a passive leg and a 6-DoF actuating hybrid limb. Actuations are completely isolated and installed on the robot frame, to reduce the moment of inertia. Legs of this type could also be realized using a 5- or 4-DoF hybrid limb (last two rows in Table 22). Figure 11 shows a hexapod prototype of the authors' research team, using T-H legs. The rotational input of this kind of leg is generated by screws and linkages, protected in the bodyshell.

7 Conclusions

(1) Two main types of walking robot legs are proposed. Type R fits omnidirectional moving platforms while type T plays a role of biomimetic mechanism.
(2) A decoupled solving method of number synthesis equation in GF set theory is proposed, which uses combinatorics to get the solution for both actuation part and constraint part.
(3) Reasonable application of GF set rules is presented to narrow the search range and successfully derives all the fifty-one kinds of walking robot legs, which could be combined to form various robots of practical value.
(4) The proposed design results are illustrated with 3D models and corresponding real prototypes, which show the practical validity of the design method.

Additional File

Additional file 1. Experimental video.

Authors' contributions
DX conceived the basic idea, designed the study and drafted the manuscript. FG provided the fundamental theory used in this paper. Both authors read and approved the final manuscript.

Authors' Information
Da Xi, born in 1989, is currently a Ph.D. candidate at *State Key Laboratory of Mechanical System and Vibration, Shanghai Jiao Tong University, China*. He received his bachelor degree from *Shanghai Jiao Tong University, China*, in 2012. His research interests include parallel mechanism and legged robots. Feng Gao, born in 1956, is currently a professor at *Shanghai Jiao Tong University, China*. His main research interests include parallel robots, design theory and its applications, large scale and heavy payload manipulator design, large scale press machine design and optimization, design and manufactory of nuclear power equipment, legged robots design and control.

Competing interests
The authors declare that they have no competing interests.

Ethics approval and consent to participate
Not applicable.

Funding
Supported by National Natural Science Foundation of China (Grant Nos. U1613208, 51335007), National Basic Research Program of China (973 Program, Grant No. 2013CB035501), Science Fund for Creative Research Groups of the National Natural Science Foundation of China (Grant No. 51421092), and Science and Technology Commission of Shanghai-based "Innovation Action Plan" Project (Grant No. 16DZ1201001).

Publisher's Note

Received: 10 May 2016 Accepted: 15 January 2018
Published online: 27 February 2018

References

1. R Playter, M Buehler, M Raibert. BigDog. *Proceedings of the SPIE Unmanned Systems Technology VIII*, Orlando, Florida, USA, April 17, 2006. Orlando: SPIE, 2006: 623020.
2. M Raibert, K Blankespoor, G Nelson, et al. Bigdog, the rough-terrain quadruped robot. *Proceedings of the 17th World Congress. The International Federation of Automatic Control*, Seoul, Korea, July 6–11, 2008, 41(2): 10822–10825.
3. X S Shao, Y P Yang, Y Zhang, et al. Trajectory planning and posture adjustment of a quadruped robot for obstacle striding. *Proceedings of the 2011 IEEE International Conference on Robotics and Biomimetics*, Phuket, Thailand, December 7–11, 2011: 1924–1929.
4. W Wang, Y P Yang. Turning maneuvers and mediolateral reaction forces in a quadruped robot. *Proceedings of the 2011 IEEE International Conference on Robotics and Biomimetics*, Phuket, Thailand, December 7–11, 2011: 515–520.
5. X B Chen, F Gao, C K Qi, et al. Spring parameters design for the new hydraulic actuated quadruped robot. *Journal of Mechanisms and Robotics*, 2014, 6(2): 021003.
6. X B Chen, F Gao, C K Qi, et al. Gait planning for a quadruped robot with one faulty actuator. *Chinese Journal of Mechanical Engineering*, 2015, 28(1): 11–19.
7. M Schilling, J Paskarbeit, T Hoinville, et al. A hexapod walker using a heterarchical architecture for action selection. *Frontiers in Computational Neuroscience*, 2013, 7: 126.
8. G Lee, S Yoo, H Shim, et al. Kinematic walking and posture control of CR200 for subsea exploration in high tidal current. *2013 OCEANS-San Diego*, San Diego: IEEE, 2013: 1–6.
9. B H Jun, P M Lee, Y H Jung. Experience on underwater artefact search using underwater walking robot Crabster CR200. *OCEANS 2015-MTS/IEEE*, Washington: IEEE, 2015: 1–5.
10. B H Jun, H Shim, B Kim, et al. Development of seabed walking robot CR200. *OCEANS-Bergen, 2013 MTS/IEEE*, Bergen: IEEE, 2013: 1–5.
11. J Y Kim, B H Jun. Design of six-legged walking robot, Little Crabster for underwater walking and operation. *Advanced Robotics*, 2014, 28(2): 77–89.
12. Y Pan, F Gao. A new 6-parallel-legged walking robot for drilling holes on the fuselage. *Proceedings of the Institution of Mechanical Engineers, Part C: Journal of Mechanical Engineering Science*, 2013: 0954406213489068.
13. Y Pan, F Gao. Payload capability analysis of a new kind of parallel leg hexapod walking robot. *Proceedings of the 2013 International Conference on Advanced Mechatronic Systems*, Luoyang, China, September 25–27, 2013. Luoyang: IEEE, 2013: 541–544.
14. Y Pan, F Gao, C K Qi, et al. Human-tracking strategies for a six-legged rescue robot based on distance and view. *Chinese Journal of Mechanical Engineering*, 2016: 1–12.
15. D L Chen, Q Liu, L T Dong, et al. Effect of spine motion on mobility in quadruped running. *Chinese Journal of Mechanical Engineering*, 2014, 27(6): 1150–1156.
16. J T Lei, H G Yu, T M Wang. Dynamic bending of bionic flexible body driven by pneumatic artificial muscles (PAMs) for spinning gait of quadruped robot. *Chinese Journal of Mechanical Engineering*, 2016, 29(1): 11–20.
17. M H Raibert, H B Brown, M Chepponis. Experiments in balance with a 3D one-legged hopping machine. *The International Journal of Robotics Research*, 1984, 3(2): 75–92.
18. R D Quinn, G M Nelson, R J Bachmann, et al. Insect designs for improved robot mobility. *Climbing and Walking Robots: From Biology to Industrial Applications*, 2001: 59.
19. J J Yu, J S Dai, S S Bi, et al. Type synthesis of a class of spatial lower-mobility parallel mechanisms with orthogonal arrangement based on Lie group enumeration. *Science China Technological Sciences*, 2010, 53(2): 388–404.
20. G Gogu. *Structural synthesis of parallel robots*. Dordrecht: Springer, 2008.
21. Z Huang, Q Li, H Ding. *Theory of parallel mechanisms*. Netherlands: Springer Netherlands, 2013.
22. F Gao, W Li, X Zhao, et al. New kinematic structures for 2-, 3-, 4-, and 5-DOF parallel manipulator designs. *Mechanism and Machine Theory*, 2002, 37(11): 1395–1411.
23. F Gao, Y Zhang, W Li. Type synthesis of 3-DOF reducible translational mechanisms. *Robotica*, 2005, 23(02): 239–245.
24. P Yang, F Gao. Kinematical model and topology patterns of a new 6-parallel-legged walking robot. *ASME 2012 International Design Engineering Technical Conferences and Computers and Information in Engineering Conference*, Chicago, Illinois, USA, August 12–15, 2012: 1197–1205.
25. X D Meng, F Gao, J L Yang. The GF sets: a new kind of performance criterion of mechanisms. *ASME 2012 International Design Engineering Technical Conferences and Computers and Information in Engineering Conference*, Chicago, Illinois, USA, August 12–15, 2012: 559–564.
26. J He, F Gao, X D Meng, et al. Type synthesis for 4-DOF parallel press mechanism using GF set theory. *Chinese Journal of Mechanical Engineering*, 2015, 28(4): 851–859.
27. M H Raibert. Trotting, pacing and bounding by a quadruped robot. *Journal of Biomechanics*, 1990, 23: 7983–8198.
28. C Semini, N G Tsagarakis, E Guglielmino, et al. Design of HyQ—a hydraulically and electrically actuated quadruped robot. *Proceedings of the Institution of Mechanical Engineers, Part I: Journal of Systems and Control Engineering*, 2011: 0959651811402275.
29. X D Meng, F Gao, Q J Ge. Number synthesis of parallel robotic mechanisms. *Mechanics Based Design of Structures and Machines*, 2014, 42(2): 211–228.
30. L K Hua. *Introduction to number theory*. Berlin: Springer Science & Business Media, 2012.
31. M Clausen, A Fortenbacher. Efficient solution of linear Diophantine equations. *Journal of Symbolic Computation*, 1989, 8(1): 201–216.
32. W S Anglin, J Lambek. Linear diophantine equations. In: *The Heritage of Thales*. New York: Springer New York, 1995: 233–235.
33. F Gao, J L Yang. *Topology synthesis for parallel robotic mechanisms*. Warsaw: Center for Advanced Studies, Warsaw University of Technology, 2013.
34. X D Meng, F Gao. The classification of GF sets for robotic mechanisms. *Proceedings of the 14th IFToMM World Congress*, Taiwan, China, October 25–30, 2015: 145–153.
35. C Gosselin. Stiffness mapping for parallel manipulators. *IEEE Transactions on Robotics and Automation*, 1990, 6(3): 377–382.
36. A Pashkevich, A Klimchik, D Chablat. Enhanced stiffness modeling of manipulators with passive joints. *Mechanism and Machine Theory*, 2011, 46(5): 662–679.
37. Y L Xu, F Gao, Y Pan, et al. Method for six-legged robot stepping on obstacles by indirect force estimation. *Chinese Journal of Mechanical Engineering*, 2016, 29(4): 1–11.